7. Develop a relationship between the precipitable water through the entire vertical extent of the atmosphere and the sea surface temperature, T_0. Assume:
a) the vertical profile of specific humidity, q_v, has the following form:
$q_v = q_0(p/p_0)\mathcal{H}_0$, where $\mathcal{H}_0$ is the surface air relative humidity;
b) the saturated vapor pressure can be approximated by the following expression:
$e_s \sim b \exp[a(T_s - T_0)]$; and
c) the specific humidity can be approximated by the water vapor mixing ratio.

8. A crude estimate of the surface moisture flux from evaporation, $\dot{E}_0$, over a large, homogeneous body of water is given by

$$\dot{E}_0 = \rho_a C_q u_x (q_0 - q_a)$$

where ρ_a is density, $C_q = 1.3 \times 10^{-3}$ (dimensionless), and u_x is wind speed. Subscripts a and 0 represent values at 10 m above the surface and the surface value, respectively. Calculate $\dot{E}_0$ under the following conditions: $u_x = 5$ m s^{-1}, $p_a = 1000$ hPa, $q_a = 20$ g kg^{-1} and $T_0 = 30$°C (assume that q_0 corresponds to saturation) and compare for the following situations:
a) a "fresh water" lake;
b) the ocean with $s = 35$ psu.

9. Calculate and compare the freezing temperature of seawater for $s = 30$ psu determined using the following:
a) theoretical value assuming an ideal, nonelectrolytic solution (4.57);
b) theoretical value assuming an electrolytic solution (4.58);
c) empirical relationship (4.59).

10. Your city has 10 km of streets, each 8 m wide. A snowfall equivalent to a sheet of ice 2 cm thick has fallen, and the temperature is –5°C. How much salt is required to melt all of the ice on the city streets?

Chapter 5 | Nucleation and Diffusional Growth

In Chapter 4, equilibrium between the phases of water was examined. In the case of condensation, it was implied that an excess of vapor pressure over the equilibrium value would cause condensation to occur, with a net migration of water molecules from the vapor to the liquid phase. In the example shown in Figure 4.5, a net migration of molecules occurred between two existing bulk phases.

In this chapter, we consider *nucleation*, a process whereby a stable element of a new phase first appears within the initial or "parent" phase. Phase transition does not occur under conditions of thermodynamic equilibrium, since a strong energy barrier must be surmounted for a phase to be nucleated if the new phase has higher atomic order than the parent phase. The energy barrier arises when a surface must be formed between the two phases.

Homogeneous nucleation refers to nucleation of a pure phase of one component. *Heterogeneous nucleation* refers to nucleation that occurs in the presence of a foreign substance, which can reduce the energy barrier to nucleation. Most of the nucleation processes in the atmosphere and the ocean occur through heterogeneous nucleation. The specific nucleation processes of interest here are the nucleation of water drops from water vapor, the nucleation of ice crystals from water drops or from vapor, and the nucleation of ice crystals in seawater to form the initial sea ice cover.

Once a phase has been nucleated, it can undergo diffusional growth if environmental conditions are favorable. Diffusion of water vapor to a cloud drop or ice crystal results in growth by condensation and deposition, respectively. Diffusional cooling of the initial sea ice cover causes further growth of the sea ice.

5.1 Surface Tension

In contrast to gases, which expand to fill the volume of their container, condensed phases can sustain a free boundary, or *surface*, and occupy a definite volume. The interface between a liquid and its vapor is not a surface in the mathematical sense, but rather a zone that is several molecules thick, over which the concentration of water molecules varies continuously.

A molecule at the surface of a liquid is free to move along the surface or into the interior of the liquid, in which case its place on the surface is taken by another molecule. However, a molecule cannot move freely from the interior of the liquid to the surface. The water molecules that form the free surface of a body of water are subjected to intermolecular attractive forces exerted by the neighboring liquid water molecules just beneath the surface. Therefore, the force field surrounding a molecule at the surface of a liquid is not symmetrical, and the molecule experiences a net force from the other molecules towards the interior of the liquid (Figure 5.1). If the surface area is increased, for example by changing the shape of the container, water molecules must be moved from the interior to the surface. To move a molecule from the interior to the surface of the liquid, work must be done against the intermolecular forces. The energy of a molecule at the surface of a liquid is thus higher than the energy in the interior. We can therefore consider the formation of a liquid surface as representing an increase in potential energy. For bulk water, such as the liquid in a drinking glass, the surface tension is a negligible part of the total potential energy, and the surface is flat rather than curved. The surface potential energy is a significant fraction of the total potential energy for small drops, since they have a large surface-to-volume ratio and curvature. A sphere has the smallest surface area for a given volume, and hence the smallest surface energy. The spherical shape of cloud drops is a consequence of the minimum-energy principle (Section 2.7).

We can extend the thermodynamic equations to include surface effects with the introduction of *surface tension work*, W_{st}. For the work required to extend a liquid surface against its vapor, we can write

$$dW_{st} = \sigma\, dA \tag{5.1}$$

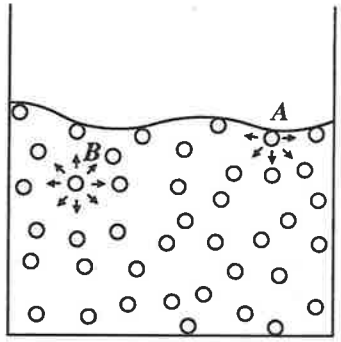

Figure 5.1 Water molecules at the surface of a liquid are subjected to a different attractive force field than those in the interior. A surface molecule, A, experiences a net attractive force towards the interior of the liquid. An interior molecule, B, experiences a symmetric force field exerted by its neighboring molecules and therefore does not freely move to the surface.

where dA is the change in surface area and σ is the *surface tension* between two phases. The surface tension is defined as the surface potential energy per unit surface area. The augmented form of the combined first and second laws for a thermodynamic system for which the surface energy is significant can be written in terms of the Gibbs function as[1]

$$dG = -\eta dT + V dp + \sigma dA \tag{5.2}$$

5.2 Nucleation of Cloud Drops

A small fraction of collisions between water vapor molecules in the atmosphere are inelastic, leading to the formation of molecular aggregates (Section 4.1). The size of an aggregate can be increased by inelastic collisions between molecular aggregates, or by accretion of individual molecules. Most aggregates have a short lifetime, since they disintegrate under continual molecular bombardment. When an aggregate attains a size sufficient for survival, then nucleation of a water drop has occurred.

To nucleate an embryo drop, energy must be supplied to form the drop surface. This energy comes from the latent heat of condensation. A water drop can be nucleated when the incremental change of surface potential energy associated with condensing new water is less than the latent heat associated with condensation. Surface tension work is proportional to the surface area of the drop ($\propto r^2$) and latent heat release is proportional to the mass of the drop ($\propto r^3$). This implies the existence of a critical radius where surface tension work and latent heat release are in balance; this critical radius thus represents the threshold for nucleation.

Because of surface tension effects, the escaping tendency of the water molecules in a spherical drop is reduced, and equilibrium vapor pressure over a spherical drop can be substantially greater than values derived for bulk water without significant surface tension effects. The higher value of saturation vapor pressure over a curved surface relative to a bulk flat surface at the same temperature is a consequence of the work that must be performed on the system to increase the drop's surface area.

For a drop with surface area $A = 4\pi r^2$, the surface tension work is determined from (5.1) to be

$$dW_{st} = \sigma_{lv} 8\pi r\, dr \tag{5.3}$$

where σ_{lv} is the surface tension between the liquid and vapor phases. Since the work

[1] Strictly speaking, since the surface tension is a change in work potential, it is defined in terms of the Helmholtz function. However, the interpretation of $\sigma = dG/dA$ is generally accepted but it cannot be demonstrated in a thermodynamically rigorous manner.

of expansion against a difference in pressure must equal the work done in changing the surface drop area,

$$\sigma_{lv}\,dA = \Delta p\,dV \tag{5.4}$$

where Δp is the pressure differential between the external ambient pressure and the internal pressure of the drop. For a spherical drop, we can write

$$\sigma_{lv}\,8\pi r\,dr = \Delta p\,4\pi r^2\,dr \tag{5.5}$$

or

$$\Delta p = \frac{2\sigma_{lv}}{r} \tag{5.6}$$

Note that the smaller the drop, the larger the pressure differential. Under standard atmospheric conditions, the internal pressure of a drop with 1 μm radius is 1.5 atm. The existence of this excess internal pressure in a small drop is a fundamental consequence of the surface tension.

The surface tension for the vapor–liquid interface of water, σ_{lv}, is a function of temperature and is given by

$$\sigma_{lv} = 0.0761 - 1.55\times 10^{-4}T \tag{5.7}$$

where σ_{lv} is in N m^{-1} and T is in °C. The expression in (5.7) is accurate for terrestrial temperatures; for higher temperatures (e.g., near the critical temperature), a higher-order polynomial expression is needed to obtain accurate values. Note that $\sigma_{lv} = 0$ at T = 374°C; this is defined as the critical temperature of water (Section 4.2).

To determine the conditions for nucleation of a water drop, we use (4.7) and (5.2) to write the Gibbs function

$$dG = -\eta\,dT + V\,dp + \sigma_{lv}\,dA + \mu_l\,dn_l + \mu_v\,dn_v \tag{5.8}$$

If we assume that nucleation occurs at constant temperature and pressure, and that $dn_l = -dn_v$, we have

$$dG = \sigma_{lv}\,8\pi r\,dr + \left(\mu_l - \mu_v\right)dn_l \tag{5.9}$$

where we have incorporated (5.3).

Since dG is an exact differential, we can consider nucleation to occur in two stages: first, the bulk condensation of supersaturated water vapor onto a plane surface; and

second, the formation of drops from the bulk water. For the first stage, we can write (5.9) as

$$dG = \left(\mu_l - \mu_v\right)dn_l$$

The term $(\mu_l - \mu_v)$ can be evaluated as follows. For an isothermal process involving one mole of water vapor, we can write

$$d\mu_v = dG = R^*T\,d\left(\ln e\right)$$

or

$$\mu_v = \mu_v^0 + R^*T\ln\frac{e}{e_0}$$

where μ_v^0 is a reference chemical potential that varies only with temperature and e_0 is the corresponding reference vapor pressure. At saturation, we can write

$$d\mu_{vs} = dG = R^*T\,d\left(\ln e_s\right)$$

and

$$\mu_{vs} = \mu_v^0 + R^*T\ln\frac{e_s}{e_0}$$

Since $\mu_l = \mu_{vs}$ when the two phases are in equilibrium over a plane surface, we can therefore write

$$\mu_l - \mu_v = R^*T\ln\left(\frac{e_s}{e}\right) \tag{5.10}$$

The number of moles of water vapor, dn_v, that condense onto spherical drops can be written

$$dn_v = \frac{1}{M_v}\,dm_v = \frac{\rho_l}{M_v}\,4\pi r^2\,dr \tag{5.11}$$

Substitution of (5.10) and (5.11) into (5.8) yields

$$dG = \left(-R_vT\ln\frac{e}{e_s}\,\rho_l\,4\pi r^2 + \sigma_{lv}\,8\pi r\right)dr \tag{5.12}$$

Integration of (5.12) for the nucleation process gives

$$\Delta G = 4\pi r^2 \sigma_{lv} - \frac{4}{3}\pi r^3 \rho_l R_v T \ln \mathcal{S} \tag{5.13}$$

where $\mathcal{S} = e_s(r)/e_s$ is the *saturation ratio* and e_s is the saturated vapor pressure over a plane surface (4.31), (4.33).

Equation (5.13) is illustrated in Figure 5.2 by plotting ΔG versus r for several different values of $\mathcal{S}$ at constant temperature. It is seen that each constant $\mathcal{S}$ curve has a maximum at radius, r^*, corresponding to the critical saturation ratio, $\mathcal{S}^*$. For a drop to grow when $r < r^*$, ΔG must be added to the drop by increasing $\mathcal{S}$. However, if $r > r^*$, as r increases then ΔG decreases and the drop grows spontaneously without increasing $\mathcal{S}$. Since in the atmosphere $\mathcal{S}$ cannot usually continue to increase, cloud drops generally grow only if they have attained a size of r^*. If the drop can reach r^* (the peak of the ΔG curve), a slight addition of molecules allows the drop to grow spontaneously. When $r = r^*$, the incremental change of surface potential energy associated with condensing new water is equal to the latent heat associated with condensation. At this point, nucleation occurs. Note from Figure 5.2 that smaller values of $\mathcal{S}^*$ are associated with larger values of r^*. As the saturation ratio increases, the energy peak (or "barrier") is lower and the value of r^* is larger.

Values of the critical radius r^* can be found by differentiating (5.13) with respect to r and setting the derivative equal to zero:

$$\left[\frac{d(\Delta G)}{dr}\right]_{T,\mathcal{S}} = \sigma_{lv} 8\pi r^* - 4\pi r^{*2} \rho_l R_v T \ln \mathcal{S} = 0$$

Solving for r^* yields

$$r^* = \frac{2\sigma_{lv}}{\rho_l R_v T \ln \mathcal{S}} \tag{5.14a}$$

We can write equivalently

$$\ln \mathcal{S} = \frac{2\sigma_{lv}}{\rho_l R_v T r^*} \tag{5.14b}$$

or

$$e_s(r) = e_s \exp\left(\frac{2\sigma_{lv}}{\rho_l R_v T r^*}\right) \tag{5.14c}$$

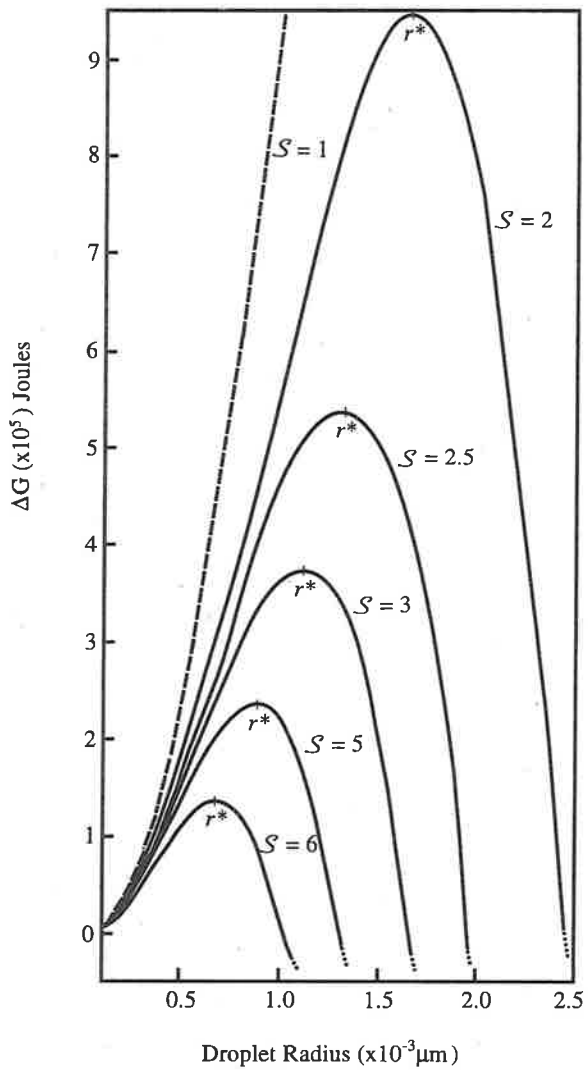

Figure 5.2 ΔG vs. r for several values of $\mathcal{S}$ at constant temperature. Each curve represents an energy barrier to embryo growth for a particular supersaturation. For radii less than the critical radius (i.e., $r < r^*$), growth occurs only by increasing $\mathcal{S}$. However, if a drop can reach the critical radius, a slight addition of molecules will push the drop over the barrier into the region where $r > r^*$. In this region, the drop can grow spontaneously, since an increase in r is accompanied by a decrease in the Gibbs energy. Note that higher values of $\mathcal{S}$ correspond to lower Gibbs energy peaks, as expected. (From Byers, 1965.)

Equations (5.14) are different forms of *Kelvin's equation*. A plot of $\mathcal{S}$ versus r^* is shown in Figure 5.3, the curve representing the critical radius for nucleation as a function of the saturation ratio. If the saturation ratio in the environment remains constant, a drop with a radius above the curve will grow spontaneously since its equilibrium vapor pressure will remain lower than the vapor pressure of its environment. A drop with radius below the curve will evaporate. Figure 5.3 shows that values of saturation ratio of order $\mathcal{S} = 3$ (corresponding to $\mathcal{H} = 300\%$) are required for the homogeneous nucleation of water drops. These high values of $\mathcal{S}$ imply a significant barrier to homogeneous nucleation of water drops in the atmosphere. Values of *supersaturation* $(\mathcal{S} - 1)$ are rarely observed to exceed 1% in the atmosphere. Homogeneous nucleation of water drops is not possible under these conditions, and we must look to heterogenous nucleation to understand nucleation of cloud drops in the atmosphere.

In the atmosphere, cloud drops form by heterogeneous nucleation. Some aerosol particles are *hygroscopic*; that is, they "attract" water vapor molecules to their surface through chemical processes or through physical forces such as those caused by the presence of permanent dipoles. A hygroscopic aerosol particle can *deliquesce* into a saturated salt solution at relative humidities signifcantly below 100%. For example, at $T = 25°C$, the deliquescent point of NaCl is about $\mathcal{H} = 75\%$ and that for $(NH_4)_2SO_4$ (ammonium sulfate) is $\mathcal{H} = 80\%$. *Cloud condensation nuclei* (CCN) are a subset of hygroscopic aerosol particles that nucleate water drops at supersaturations less than 1%. Soluble particles such as NaCl and $(NH_4)_2SO_4$ lower the equilibrium vapor pressure of a water solution relative to pure water (Section 4.5) and thus partially counteract the effects of surface tension. There are both natural and anthropogenic sources of CCN. Sulfate particles are produced anthropogenically by the burning of sulfur-containing fuels. Volcanic eruptions are also a source of sulfate particles.

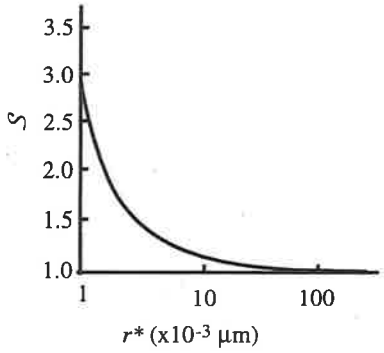

Figure 5.3 Equilibrium saturation ratio for pure water drops as a function of radius. Values are calculated from the Kelvin equation (5.14). The curve represents an unstable equilibrium. A drop above the equilibrium curve will grow, while a drop below the equilibrium curve will evaporate.

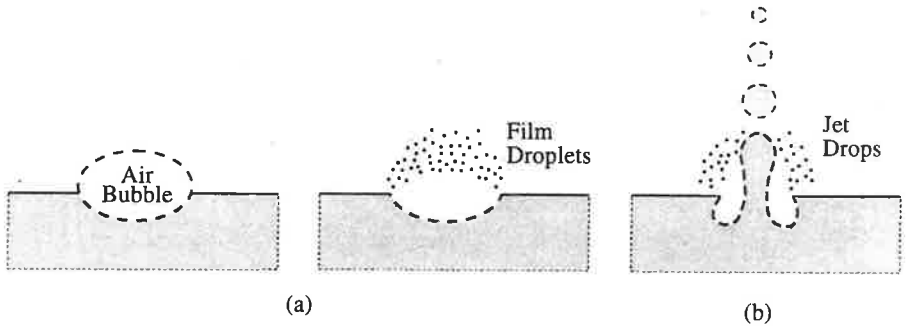

Figure 5.4 Production of sea-salt aerosols from (a) bursting air bubbles on the surface of the ocean and (b) mechanically breaking surface waves.

The ocean is a source of two types of aerosol important for the condensation of water in the atmosphere. Air bubbles at the surface of the ocean burst, ejecting small drops into the atmosphere (Figure 5.4). After evaporation these drops leave behind sea-salt particles with diameters smaller than about 0.3 μm. When air bubbles in breaking waves burst, larger drops are ejected in jets; upon evaporation of the drops, giant sea-salt particles (>2 μm) may be left in the atmosphere. It has been estimated that the rate of production of sea-salt aerosol particles over the oceans by this mechanism is 100 $cm^{-2}\ s^{-1}$.

An additional source mechanism of aerosols from the oceans is associated with organosulfides produced by micro-organisms in the ocean. In particular, the compound dimethylsulfide (DMS; $(CH_3)_2S$) is produced by marine phytoplankton in the upper layers of the ocean and represents the major flux of reduced sulfur to the marine atmosphere. Since DMS is rather volatile and insoluble, it passes rapidly from the seawater into the atmosphere. Once in the atmosphere, DMS is oxidized and forms sulfate particles.

The number of CCN per unit volume of air that have critical supersaturation values less than $(\mathcal{S}-1)$ is approximated by

$$N_{CCN} = c_1(\mathcal{S} - 1)^k \tag{5.15}$$

where c_1 and k are parameters that depend on the particular air mass. Maritime conditions have values that are typically $c_1 = 50\ cm^{-3}$ and $k = 0.4$, whereas continental conditions have typical values around $c_1 = 4000\ cm^{-3}$ and $k = 0.9$ (for $\mathcal{S}-1$ in %). Urban regions have exceptionally large numbers of CCN. The fraction of the total atmospheric aerosol population that serve as CCN in clouds is about 1% of the total aerosol population in continental regions and up to 20% of the total aerosol concentration over the ocean.

Recall Raoult's law from Section 4.5 for an electrolytic solution (4.48):

$$\frac{e_s(n_{solt})}{e_s} = 1 - \frac{\varepsilon n_{solt}}{n_{H_2O}}$$

Since $n = m/M$, we can write for a solution drop

$$\frac{e_s(n_{solt})}{e_s} = 1 - \frac{3\varepsilon m_{solt} M_v}{4\pi M_{solt} \rho_l r^3} = 1 - \frac{b}{r^3} \tag{5.16a}$$

where

$$b = 3\varepsilon M_v \frac{m_{solt}}{4\pi M_{solt} \rho_l} \tag{5.16b}$$

For a given mass of solute, the vapor pressure required for equilibrium decreases as the cube of the drop radius. As r increases through condensation, the mole fraction of the solute decreases. Thus the depression of the equilibrium vapor pressure for a given mass of solute decreases as r increases.

Combination of the curvature (5.14c) and the surface tension (5.16) effects on saturation vapor pressure gives the ratio of the saturation vapor pressure of a solution drop to the saturation vapor pressure of pure water over a flat surface:

$$\frac{e_s(r,m_{solt})}{e_s} = \left(1 - \frac{b}{r^3}\right) \exp(a/r) \tag{5.17}$$

where $a = 2\sigma_{lv}/(\rho_l R_v T)$. If r is not too small, (5.17) can be written as

$$\frac{e_s(r,n_{solt})}{e_s} = 1 + \frac{a}{r} - \frac{b}{r^3} \tag{5.18}$$

For given values of T, M_{solt}, and m_{solt}, (5.18) describes the dependence of saturation ratio on the size of the solution drop.

Equilibrium curves for drops containing a given nucleus mass (referred to as *Kohler curves*) are shown in Figure 5.5. Depending on whether the solute or curvature effect dominates, the saturation ratio may be greater or less than unity. The peaks in the Kohler curves correspond to critical values of the supersaturation and radius, $\mathcal{S}^*$ and r^*. For $r < r^*$, the drops grow only in response to an increase in relative humidity, and are termed *haze particles*. A condensation nucleus is said to be *activated* when the drop formed on it grows to size r^*. Once the drop grows only slightly beyond r^*, its equilibrium value of $\mathcal{S}$ is less than $\mathcal{S}^*$, and the drop grows spontaneously without requiring further increase in $\mathcal{S}$. For typical sizes of condensation nuclei found in the atmosphere, the critical supersaturation for heterogeneous nucleation on a soluble particle is less than 1% (Table 5.1), in agreement with observations.

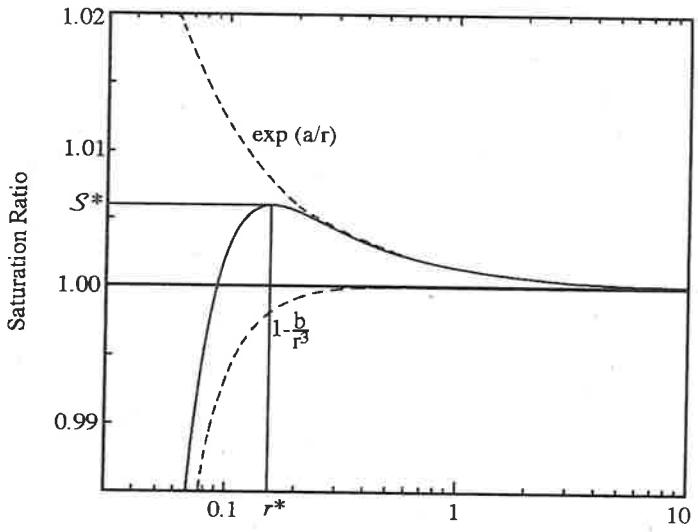

Figure 5.5 Equilibrium saturation ratio for a solution drop as a function of drop radius. The solution effect ($1-b/r^3$) dominates when the radius is small. For values of $r < r^*$, drop growth occurs only in response to an increase in the relative humidity. If the relative humidity at the critical radius slightly exceeds the critical saturation ratio, then the drop can grow spontaneously, and will continue to grow as long as the ambient saturation ratio remains higher than the equilibrium saturation ratio of the drop.

Table 5.1 Critical values of radius and supersaturation for typical condensation nuclei in the atmosphere (values assume that the nuclei are NaCl and that the temperature is 273 K).

m_{nuclei} (g)	r_{nuclei} (μm)	r^* (μm)	$\mathcal{S}^*-1$ (%)
10^{-16}	0.0223	0.19	0.42
10^{-15}	0.0479	0.61	0.13
10^{-14}	0.103	1.9	0.042
10^{-13}	0.223	6.1	0.013
10^{-12}	0.479	19.0	0.0042

5.3 Nucleation of the Ice Phase

Nucleation of ice in the atmosphere may occur from supersaturated vapor (deposition) or from supercooled water (freezing). While the theory of liquid water nucleation from the vapor phase is fairly well established, there is considerable controversy over the mechanisms of ice nucleation in the atmosphere.

Pure bulk water is not observed to exist in the liquid phase at temperatures significantly below 0°C. However, when water is divided into small drops, its freezing temperature is observed to become much lower. The smaller the drop, the lower the statistical probability that it will freeze at a given temperature since there are fewer water molecules from which to form a stable, ice-like structure. Analogous to (5.14a), an expression for critical radius for homogenous ice nucleation from a liquid water drop can be derived:

$$r^* = \frac{2\sigma_{il}}{\rho_i R_v T \ln\left(\frac{e_s}{e_{si}}\right)} \tag{5.19}$$

where σ_{il} is the surface tension at the ice-liquid interface. Using the Clausius–Clapeyron equation (4.31), it can be shown that (following McDonald, 1964)

$$r^* = \frac{2\sigma_{il} T_{tr}}{\rho_i \overline{L_{il}}\left(T_{tr} - T\right)} \tag{5.20}$$

where the subscript i refers to ice, $T_{tr} = 273.15$ K is the nominal freezing temperature of bulk water, and $\overline{L_{il}}$ represents the average latent heat of fusion over the temperature range T to T_{tr}. The numerical value of σ_{il} is known approximately to be about 0.002 N m^{-1}. Table 5.2 shows typical homogeneous freezing temperatures of water drops. Small drops of pure water freeze at a temperature of about –40°C. Equation (5.20) agrees with observations to within 2°C.

The homogeneous nucleation of ice from a pure supercooled water drop in the atmosphere is not possible, since cloud drops contain at least one CCN. In accordance with (4.65), the freezing temperature of a solution is depressed relative to pure water. However, as a drop grows, the solution becomes increasingly dilute. In the upper troposphere, temperatures reach –40°C and colder. Therefore, homogenous freezing nucleation of dilute solution drops is believed to be the primary nucleation mechanism for cirrus clouds.

Most clouds contain ice particles by the time the temperature has reached –20°C, indicating the importance of heterogeneous ice nucleation. The class of aerosols that act as condensation nuclei and those that act as ice nuclei are almost mutually exclusive. CCN particles are soluble in water, promoting nucleation by lowering the saturation vapor pressure. In contrast, ice nuclei promote nucleation by providing a

Table 5.2 Typical homogeneous freezing temperatures of water drops. (Data from Young, 1993.)

Drop diameter (μm)	T_f (°C)
1	–42.3
10	–38.2
100	–34.8
1,000	–32.2
10,000	–30.0

substrate upon which the ice lattice can form. For an aerosol to be an effective ice nucleus, some combination of lattice matching, molecular binding, and low interfacial energy with ice is needed. Soil particles, particularly clay minerals, are effective ice nuclei since their lattice structure is similar to that of ice. Anthropogenic sources of ice nuclei include by-products of combustion and smelting, such as metallic oxides. Biogenic ice nuclei consist of bacterial cells, and sources from leaves and the ocean have been identified. Biogenic ice nuclei possess hydrogen bonding capability, with positions of the hydrogen bonding sites matching those found in ice.

Four different types of heterogeneous ice nucleation have been hypothesized: deposition nucleation, immersion freezing, contact freezing, and condensation freezing. *Deposition nucleation* occurs when a small amount of water is adsorbed on the surface of a nucleus and freezes, then additional water vapor is deposited. *Immersion freezing* occurs when an ice nucleus is present within the drop. As the drop cools, the likelihood of nucleating an ice crystal increases. The amount of supercooling required for immersion nucleation decreases for larger sizes of nuclei. *Contact freezing* occurs when an ice nucleus makes external contact with a supercooled drop and very quickly initiates freezing. A necessary condition for contact freezing is that the aerosol particle must make contact with the drop. This contact can occur via bombardment of the aerosol particle by air molecules or by aerosol transport in a temperature or vapor gradient. *Condensation freezing* occurs when a transient water drop forms before the freezing occurs, and then freezing occurs via contact or immersion nucleation.

Table 5.3 summarizes the ice nucleation thresholds for various substances. It is seen that a particular aerosol particle may nucleate ice in different ways, depending on the history of the aerosol interaction with the cloud and the ambient temperature and humidity conditions. Given the complexity of the processes and the difficulty in making measurements, the dominant modes of heterogeneous ice nucleation in the atmosphere, and even the possible modes, remain controversial. Note the small supercooling required for ice nucleation by AgI (silver iodide) in Table 5.3. Because the crystal lattice of AgI very nearly duplicates that of ice, AgI has been used as a

Table 5.3 Comparison of the threshold temperatures for ice nucleation of various substances for various nucleation modes. Thresholds represent the highest temperatures at which ice nucleation has been observed to occur. (Following Young, 1994.)

Substance	Contact freezing	Condensation freezing	Deposition nucleation	Immersion
Silver iodide	–3	–4	–8	–13
Cupric sulfide	–6	n/a	–13	–16
Lead iodide	–6	–7	–15	n/a
Cadmium iodide	–12	n/a	–21	n/a
Metaldehyde	–3	–2	–10	n/a
1,5-Dihydroxy-naphlene	–6	–6	–12	n/a
Phloroglucinol	n/a	–5	–9	n/a
Kaolinite	–5	–10	–19	–32

cloud-seeding agent, whereby it is injected into supercooled clouds to modify the cloud microphysical processes. Cloud seeding has been attempted for precipitation enhancement and suppression, hail and lightning suppression, and the dispersal of fog. The effectiveness of cloud seeding, however, remains controversial.

Observations in some clouds show substantially larger numbers of ice crystals than expected, relative to the number of ice nuclei present. Freezing drops with radius greater than 12 μm may splinter into several ice crystals, and existing ice crystals may fracture through collisions with other ice crystals. Secondary ice crystal production is seen in clouds with large drops and large updrafts.

5.4 Diffusional Growth of Cloud Drops

Cloud drops grow by diffusion of water vapor to the drop. Water vapor is transferred to the drop by molecular diffusion as long as the vapor pressure surrounding the drop exceeds the saturation vapor pressure of the drop. As water condenses on the drop, latent heat is released, which warms the drop and reduces its growth rate. As a result of the latent heat release, the drop becomes warmer than the environment, and heat is diffused away from the drop. Condensation can thus be considered as a double diffusive process, with water vapor diffused towards the drop and heat diffused away from the drop. Evaporation of a drop occurs in reverse, as water diffuses away from the drop and heat diffuses toward the drop.

First we derive an equation for the diffusional growth of a single drop that exists in a vapor field of infinite extent. The diffusion equation for water vapor (3.42) is

$$\frac{\partial \rho_v}{\partial t} = D_v \frac{\partial^2 \rho_v}{\partial x_i^2}$$

where we assume here that D_v is not a function of x_i. For stationary (steady-state) conditions, the mass flux of water vapor, dm/dt, on a sphere of radius r is equal to the flux of vapor across the drop surface:

$$\frac{dm}{dt} = 4\pi r^2 D_v \frac{d\rho_v}{dr} \tag{5.21}$$

Integrating (5.21) from the surface of the drop to infinity (a distance from the drop sufficiently far so that the vapor pressure is unaffected by diffusion to the drop) and assuming that the growth rate, dm/dt, remains constant, we obtain

$$\frac{dm}{dt}\int_r^\infty \frac{dr}{r^2} = 4\pi D_v \int_{\rho_v(r)}^{\rho_v(\infty)} d\rho_v \tag{5.22}$$

and therefore

$$\frac{dm}{dt} = 4\pi r D_v\left[\rho_v(\infty) - \rho_v(r)\right] \tag{5.23}$$

Latent heat liberated by condensation at the drop surface is diffused away from the drop according to (3.41), and we can write analogously to (5.23)

$$\frac{dQ}{dt} = -L_{lv}\frac{dm}{dt} = 4\pi r \kappa\left[T(r) - T(\infty)\right] \tag{5.24}$$

Writing the term dm/dt in terms of a change in radius, we obtain

$$\frac{dm}{dt} = \rho_l \frac{dV}{dt} = \rho_l 4\pi r^2 \frac{dr}{dt} \tag{5.25}$$

Combination of (5.23) and (5.24) determines the drop growth rate as influenced by both diffusion of water vapor and heat. An approximate expression for the growth rate of a drop by diffusion has been determined from (5.24)–(5.26) to be (Mason, 1971):

$$r\frac{dr}{dt} = \frac{\mathcal{S}-1}{\left(\dfrac{L_{lv}^2\rho_l}{\kappa R_v T^2} + \dfrac{\rho_l R_v T}{e_s(T)D_v}\right)} = \frac{\mathcal{S}-1}{\mathcal{K}+\mathcal{D}} \tag{5.26}$$

If $\mathcal{S} < 1$, then (5.26) describes the evaporation of a cloud drop. The solution (5.26) depends only on the ambient environmental conditions ($\mathcal{S}$, T, p) and does not require determination of the drop temperature. Note that curvature and solute effects have been ignored in this derivation; their effects are small once the drop size has increased beyond a few microns.

The term $\mathcal{K}$ in (5.26) represents the thermodynamic term associated with heat conduction, and $\mathcal{D}$ is associated with the diffusion of water vapor. The coefficients of thermal conductivity and water vapor diffusivity vary with temperature, and selected values are given in Table 5.4.

Since $\mathcal{K}$ and $\mathcal{D}$ depend on the ambient temperature and pressure, (5.26) cannot be integrated analytically. If we assume that ambient conditions in the atmosphere remain constant (i.e., $\mathcal{S}$, $\mathcal{K}$ and $\mathcal{D}$ are constant), we can integrate (5.26) as

$$r(t) = \left[r_o^2 + \frac{2(\mathcal{S}-1)}{\mathcal{K}+\mathcal{D}}(t-t_o)\right]^{1/2} \tag{5.27}$$

Because of the square–root dependence, (5.27) is often called the *parabolic growth law*. Table 5.5 shows the growth rate of drops of different sizes, as determined from (5.27).

Table 5.4 Coefficients of atmospheric thermal conductivity and water vapor diffusivity at a pressure of 1000 mb (from Houghton, 1985). Since D_v varies with pressure, a value of D_v for an arbitrary pressure p (hPa) can be obtained by multiplying the tabulated value by (1000/p).

T (°C)	κ (J m^{-1} s^{-1} K^{-1}) × 10^{-2}	D_v (m^2 s^{-1}) × 10^{-5}
−40	2.07	1.62
−30	2.16	1.76
−20	2.24	1.91
−10	2.32	2.06
0	2.40	2.21
10	2.48	2.36
20	2.55	2.52
30	2.63	2.69

Table 5.5 Drop growth rate calculated from (5.26), with $r_o = 0.75$ μm. The drops are growing on nuclei of NaCl at $(\mathcal{S} - 1) = 0.05\%$, $p = 900$ mb, $T = 273$ K. (After Mason, 1971.)

Mass (g)	10^{-14}	10^{-13}	10^{-12}
Radius (μm)	Time (seconds) to grow from initial radius, r_o		
1	2.4	0.15	0.013
2	130	7.0	0.61
4	1,000	320	62
10	2,700	1,800	870
20	8,500	7,400	5,900
30	17,500	16,000	14,500
50	44,500	43,500	41,500

Smaller drops have a faster growth rate (dr/dt) than larger drops. However, large drops have a greater rate of mass buildup (dm/dt). It is clear from Table 5.5 that diffusional growth of drops is not sufficient to produce a rain drop even over a period of a half day. Additional mechanisms are required to explain the observed rapid formation of rain drops (see Section 8.2).

In natural clouds, there is not an infinite source of water vapor, and drops compete for water vapor and otherwise influence each other's growth. The rate of change of supersaturation is therefore determined as a balance between the production of supersaturation (by cooling, for example) and condensation (which decreases the ambient supersaturation). Assuming that supersaturation is produced initially by adiabatic cooling in an updraft u_z, the rate of change of the saturation ratio is given by

$$\frac{d\mathcal{S}}{dt} = \mathcal{A}_1 u_z - \mathcal{A}_2 \frac{dw_l}{dt} \tag{5.28}$$

where w_l is the liquid water mixing ratio (mass of liquid water per mass of dry air), and dw_l/dt is the rate of condensation. The term $\mathcal{A}_1 u_z$ is thus a "source" term, representing the increase of the saturation ratio due to cooling in adiabatic ascent, and $\mathcal{A}_2(dw_l/dt)$ is the "sink" term, representing the decrease in supersaturation due to the diffusion of water vapor to the growing drops.

The term $\mathcal{A}_1$ can be derived in the following way. Assuming ascent without condensation, (5.28) becomes

$$\frac{d\mathcal{S}}{dt} = \mathcal{A}_1 u_z \tag{5.29}$$

Using the definition $\mathcal{S} = e/e_s$, we can write

$$\frac{d\mathcal{S}}{dt} = \frac{\left(e_s \frac{de}{dt} - e \frac{de_s}{dt}\right)}{e_s^2} \tag{5.30}$$

Using Dalton's law of partial pressures (1.13), we can apply the hydrostatic equation (1.33) to water vapor

$$\frac{de}{dz} = -g\rho_v \tag{5.31}$$

Using the chain rule, we can write (5.31) as

$$\frac{de}{dt}\frac{dt}{dz} = -g\rho_v \tag{5.32}$$

or equivalently

$$\frac{de}{dt} = -\frac{eg}{R_v T} u_z \tag{5.33}$$

where we have incorporated the ideal gas law. The Clausius–Clapeyron equation (4.19) can be expanded using the chain rule as

$$\frac{de_s}{dt}\frac{dt}{dz}\frac{dz}{dT} = \frac{L_{lv} e_s}{R_v T^2} \tag{5.34}$$

or equivalently

$$\frac{de_s}{dt} = -\frac{L_{lv} e_s}{R_v T^2}\frac{g}{c_p} u_z \tag{5.35}$$

where $dT/dz = -g/c_p$ since no condensation has occurred. Incorporating (5.33) and (5.35) into (5.30) yields the coefficient $\mathfrak{A}_1$. An analogous procedure is used to derive $\mathfrak{A}_2$. Values of $\mathfrak{A}_1$ and $\mathfrak{A}_2$ thus derived are

$$\mathfrak{A}_1 = \frac{1}{T}\left(\frac{L_{lv} g}{R_v c_p T} - \frac{g}{R_d}\right) \tag{5.37}$$

$$\mathfrak{A}_2 = \rho_a \left(\frac{R_v T}{\varepsilon e_s(T)} + \frac{\varepsilon L_{lv}^2}{pTc_p}\right) \tag{5.38}$$

If the production of saturation ratio occurs via isobaric cooling rather than by adiabatic cooling, then

$$\frac{d\mathcal{S}}{dt} = \mathfrak{A}_3 \frac{dT}{dt} - \mathfrak{A}_4 \frac{dw_l}{dt} \tag{5.39}$$

where dT/dt is the isobaric cooling rate resulting from radiative cooling or other isobaric processes. The terms $\mathfrak{A}_3$ and $\mathfrak{A}_4$ can be shown to be

$$\mathfrak{A}_3 = -\frac{L_{lv}}{R_v T^2} \tag{5.40a}$$

$$\mathfrak{A}_4 = \frac{p}{\varepsilon e_s} \tag{5.40b}$$

By using either (5.29) or (5.39) with (5.26), and providing a distribution of CCN and an updraft velocity or an isobaric cooling rate, the evolution of a spectrum of drops can be calculated. The results of such a calculation are shown in Figure 5.6. From an initial spectrum of CCN, drops are nucleated and grow in a steady updraft. The supersaturation increases from zero at the cloud base to a maximum value of 0.5% at about 10 m above the cloud base. Above this height, $(\mathcal{S} - 1)$ decreases as condensation depletes the water vapor concentration. The peak supersaturation is not sufficient to nucleate the two smallest sizes of nuclei; they remain as haze drops, growing only when the supersaturation is increasing. The larger nuclei become activated as cloud drops, which undergo rapid growth when the supersaturation is a maximum.

The *drop size spectrum*, $n(r)$, is defined as the number of drops per unit volume of air with radii in the interval $r + dr$. The total number concentration of the drops, N, is

$$N = \int_0^\infty n(r)\, dr \tag{5.41}$$

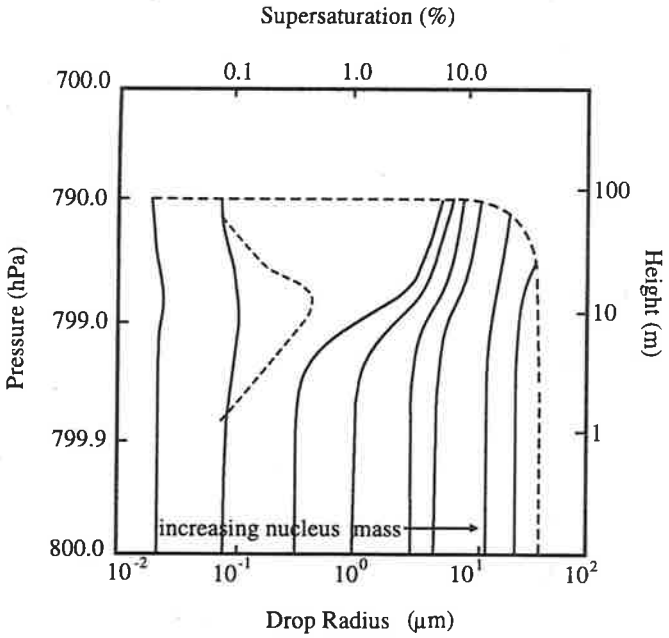

Figure 5.6 Evolution of a cloud drop spectrum from an assumed updraft velocity and initial distribution of CCN. Solid lines show the sizes of drops growing on nuclei of different masses. The dashed line shows how the supersaturation varies with height. The smallest drops grow slightly during the increase in supersaturation, but then evaporate again when the supersaturation decreases. Larger drops become activated and grow rapidly during the increase in supersaturation. (From Rogers and Yau, 1989.)

Variations in drop sizes associated with a spectrum of aerosol sizes give rise to a spectrum of drop sizes. As the activated drops grow, their spread in size becomes smaller, in accord with the parabolic growth law. Figure 5.7a shows the narrowing of the drop size spectrum with time (or with height above cloud base for drops growing in an updraft) according to the simple diffusional growth theory. Figure 5.7b shows observed drop size spectra from a shallow non-precipitating cloud. In general, observed drop size spectra are significantly broader than modeled spectra. Also, the observed drop size spectrum broadens with height above cloud base, while the simple diffusional growth model indicates a narrowing of the drop size spectrum. The discrepancy between the modeled and observed drop size spectra is of concern, because the drop size spectra is very important in formation of precipitation and in the interaction of clouds with radiation (see Sections 8.2 and 8.3).

Explaining the observed broadening of drop size spectra remains a major challenge to cloud physicists. Numerous theories have been proposed to explain the spectral broadening. For example, "giant" particles within a distribution of CCN may act as

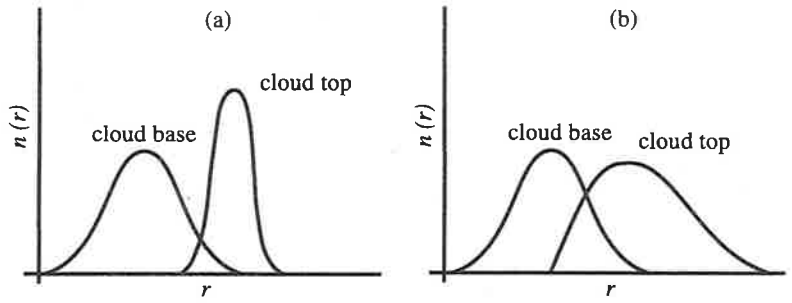

Figure 5.7 (a) Modeled cloud drop size spectra according to the simple diffusional growth model. (b) Observed spectra for a shallow, non-precipitating cloud. At cloud top, the observed spectrum is much broader than the modeled spectrum.

embryos for large drops. Another theory is that small-scale turbulence and the associated fluctuations in supersaturation may cause drop spectral broadening in some circumstances. Variations in the spatial distribution of drops may give rise to local supersaturation fluctuations and thus contribute to broadening of the drop size spectra. Entrainment of dry air into the cloud has also been hypothesized to contribute to drop spectral broadening. Because of the difficulty in making measurements at these small scales, the relative importance of each of these processes in broadening the drop spectrum by condensational growth remains uncertain.

5.5 Ice Crystal Morphology and Growth

Ice crystal growth by diffusion is regulated to a large extent by the surface properties of the ice crystal lattice. Unlike diffusional growth of a liquid water drop, water vapor molecules cannot be incorporated into the crystal lattice at their arrival position. A water vapor molecule can only be incorporated into steps or corners of the lattice, and must migrate across the crystal surface until it either reaches such a site or returns to the vapor. The necessity of incorporating incoming water molecules into the growing ice lattice reduces the growth rate of the ice crystal.

The temperature and saturation ratio are the primary influences on the *habit* assumed by a growing ice crystal, determining whether a crystal grows preferentially along the basal (*c*-axis) or the prism (*a*-axis) faces. Figure 5.8 shows various ice crystal habits. Needles occur singly or in bundles, and columnar forms include columns, pyramids, and bullets. Plates include simple hexagons, sectored hexagons, stars, and highly branched dendrites. Figure 5.9 shows the dependence of ice crystal habit on temperature and vapor density excess. Needles and columnar ice crystals represent growth primarily on the *c*-axis, while plates represent growth that has

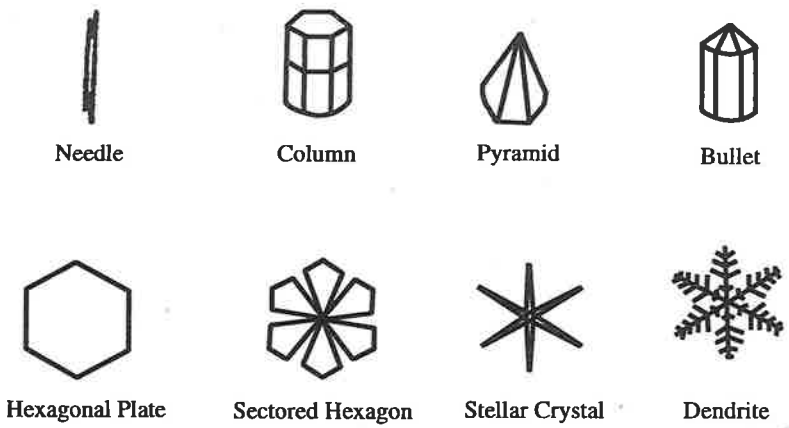

Figure 5.8 Examples of various ice crystal habits.

occurred primarily on the a-axis. Combination crystals such as columns with plates at the ends can arise from exposure to successively different ambient temperatures and humidities.

The diffusional growth of ice crystals in a water vapor field (and conversely, ice crystal sublimation) is treated in essentially the same way as the growth and evaporation of liquid water drops. In a manner analogous to that used to derive (5.26), the following equation can be derived for the growth rate of an ice crystal:

$$\frac{dm}{dt} = \frac{4\pi \mathcal{C}\left(\mathcal{S}_i - 1\right)}{\left(\dfrac{L_{iv}^2}{\kappa R_v T^2} + \dfrac{R_v T}{e_{si}(T) D}\right)} \tag{5.42}$$

In (5.41) the saturation ratio with respect to ice, $\mathcal{S}_i = e/e_{si}$, is used in place of $\mathcal{S}$, and the latent heat of sublimation replaces the latent heat of vaporization. Another difference between (5.41) and (5.26) is the appearance in (5.41) of the factor $\mathcal{C}$ instead of r. Since ice crystals are nonspherical, a radius cannot be assigned to them. The diffusion of vapor to an ice crystal can be addressed in a manner derived from an analogous situation in electricity, where the capacitance, $\mathcal{C}$, is used in dealing with irregularly shaped objects. For a sphere, $\mathcal{C} = r$. For a disk, which can be used to approximate a plate, $\mathcal{C} = 2r/\pi$. Because of kinetic effects and the nature of growth of the ice crystal lattice, the growth rate of small ice crystals in some situations may be only half the rate predicted by (5.42).

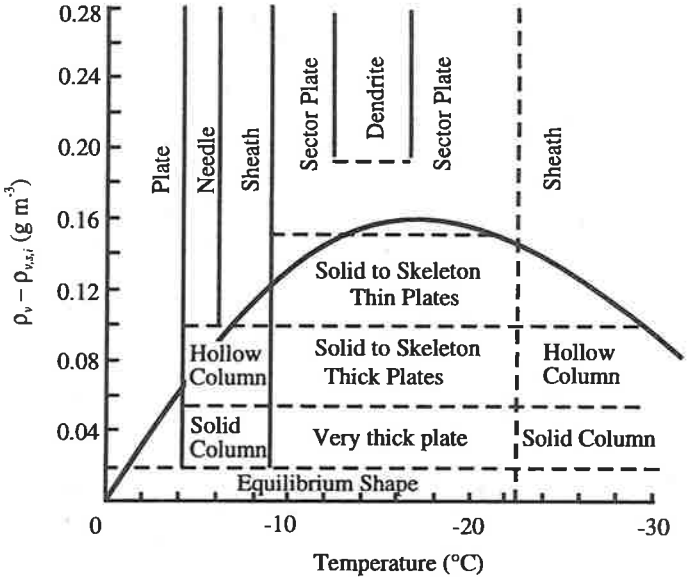

Figure 5.9 Dependence of ice crystal habit on environmental conditions. Also shown is the excess vapor density over ice equilibrium in a saturated atmospere (thick curve). Note that the excess vapor density is a maximum at around –17°C, which corresponds to the temperature at which ice crystal growth is a maximum. (From Pruppacher and Klett, 1978.)

When ice crystals first nucleate in a cloud, they are typically found in the presence of water drops, with the ambient vapor pressure approximately equal to saturation vapor pressure over liquid water. As was shown in Figure 4.4 and Table 4.4, this results in a supersaturation with respect to ice. A water-saturated cloud has a high supersaturation with respect to ice, and hence provides a very favorable environment for diffusional growth of ice crystals.

5.6 Formation of the Initial Sea Ice Cover

Nucleation of the initial ice particles in seawater in response to surface cooling occurs via heterogeneous nucleation. The sources of ice-forming nuclei are solid impurities (both organic and inorganic) that occur in seawater and also snow particles that fall onto the ocean surface. Supercooling required to form the initial ice cover probably does not exceed a few tenths of a degree Celsius.

Central to the formation of a surface ice cover on a body of fresh water is the fact that the density of the ice is less than the density of the liquid. The density of pure liquid water has a maximum value of 1000 kg m^{-3} at $T_\rho = 3.98$°C, while the density of